



Published in final edited form as:

*Acta Biomater.* 2021 September 01; 131: 222–235. doi:10.1016/j.actbio.2021.06.048.

## Development of alginate and gelatin-based pleural and tracheal sealants

**Nathan Gasek<sup>a,i,1</sup>, Heon E. Park<sup>a,b,c,1</sup>, Juan J. Uriarte<sup>a</sup>, Franziska E. Uhl<sup>a,d</sup>, Robert A. Pouliot<sup>a</sup>, Alexander Riveron<sup>e</sup>, Tovah Moss<sup>e</sup>, Zachary Phillips<sup>e</sup>, Jessica Louie<sup>d</sup>, Ishna Sharma<sup>f</sup>, Benefsha Mohammed<sup>e</sup>, Jacob Dearborn<sup>a</sup>, Patrick C. Lee<sup>b,f</sup>, Todd Jensen<sup>g</sup>, John Garner<sup>h</sup>, Christine Finck<sup>g</sup>, Daniel J. Weiss<sup>a,\*</sup>**

<sup>a</sup>Department of Medicine, University of Vermont, Burlington, VT, USA

<sup>b</sup>Department of Mechanical Engineering, University of Vermont, Burlington VT, USA

<sup>c</sup>Department of Chemical and Process Engineering, University of Canterbury, Christchurch, New Zealand

<sup>d</sup>Department of Experimental Medical Sciences, Lund University, Lund, Sweden

<sup>e</sup>Department of Surgery, University of Vermont, Burlington, VT, USA

<sup>f</sup>Department of Mechanical and Industrial Engineering, University of Toronto, Toronto, Canada

<sup>g</sup>Department of Surgery, Connecticut Children's Hospital, Hartford, CT, Department of Pediatrics, University of Connecticut School of Medicine, Farmington CT, USA

<sup>h</sup>Akina Inc., West Lafayette, IN, USA

<sup>i</sup>University of Connecticut School of Medicine, Farmington CT, USA

### Abstract

Pleural and tracheal injuries remain significant problems, and an easy to use, effective pleural or tracheal sealant would be a significant advance. The major challenges are requirements for adherence, high strength and elasticity, dynamic durability, appropriate biodegradability, and lack of cell or systemic toxicity. We designed and evaluated two sealant materials comprised respectively of alginate methacrylate and of gelatin methacryloyl, each functionalized by conjugation with dopamine HCl. Both compounds are cross-linked into easily applied as pre-formed hydrogel patches or as *in situ* hydrogels formed at the wound site utilizing FDA-approved photo-initiators and oxidants. Material testing demonstrates appropriate adhesiveness, tensile strength, burst pressure, and elasticity with no significant cell toxicity *in vitro* assessments.

\*Corresponding author at: Department of Medicine, 149 Beaumont Avenue, 226 Health Science Research Facility, University of Vermont, Burlington, VT 05405, USA. daniel.weiss@uvm.edu (D.J. Weiss).

<sup>1</sup>Denotes Co-first Authors.

#### Disclosure

This manuscript is not under consideration for publication elsewhere, its publication is approved by all authors and tacitly or explicitly by the responsible authorities where the work was carried out, and that, if accepted, it will not be published elsewhere in the same form, in English or in any other language, including electronically without the written consent of the copyright-holder.

#### Declaration of Competing Interest

There are no conflicts of interest for any participating authors.

Air-leak was absent after sealant application to experimentally-induced injuries in *ex-vivo* rat lung and tracheal models and in *ex vivo* pig lungs. Sustained repair of experimentally-induced pleural injury was observed for up to one month *in vivo* rat models and for up to 2 weeks *in vivo* rat tracheal injury models without obvious air leak or obvious toxicities. The alginate-based sealant worked best in a pre-formed hydrogel patch whereas the gelatin-based sealant worked best in an *in situ* formed hydrogel at the wound site thus providing two potential approaches. These studies provide a platform for further pre-clinical and potential clinical investigations.

## Keywords

Sealant; Lung; Pleura; Trachea; Alginate; Gelatin; Methacryloyl; Dopamine conjugation

---

## 1. Introduction

Trauma, including battlefield trauma, lung resection surgeries, and a variety of lung diseases such as emphysema, infections, and lung cancers, as well as complications of mechanical ventilation of critically ill patients in operating rooms and intensive care units, result in air (pneumothorax) or liquid (pleural effusions) leaking out of the lung. These events often result in lung collapse that can be immediately life-threatening or result in chronic air leakage (bronchopleural fistula, BPF) that can be difficult to manage. This leads to significantly increased morbidity, mortality, hospital stays, health care costs, and other complications. According to available Medicare databases, up to 0.5% of the US population is affected; > 100,000 patients per year with \$2.8 billion annual health care costs [1]. Further, pneumothorax and traumatic lung injury are estimated as the second leading cause of preventable battlefield deaths resulting in an estimated 5% of all fatal injuries [2]. In parallel, tracheobronchial tree injuries are less common but can be immediately life threatening. These defects, which result from trauma, including battlefield, disease, or are congenital, can also be difficult to manage and require invasive surgery to repair the defect. While there is less available data, neck/larynx/trachea injuries comprised 18.8% of total compiled facial and invasive neck traumatic injuries in Iraq and Afghanistan 2011–2016 [3]. Thus there is a critical need for both military and civilian approaches for acute and chronic lung and tracheal injuries.

While the concept of developing a pleural or tracheobronchial sealant is itself not novel, no compounds evaluated to date have proven clinically successful. This includes a range of materials such as fibrin, cyanoacrylates (super glue), and others [4–12]. Progel TM (Bard-Davol Inc.) is the only currently FDA-approved pleural sealant in the US. However, it is only approved for repair of surgical stumps in open surgical pulmonary resections but not for BPF or other lung injuries including trauma. Further, Progel TM is technically cumbersome to apply, contraindicated in renal failure, may cause allergic reactions, and is not approved for use in pediatric or pregnant patients [13,14]. Thus, despite recent promising initial investigations into other potential sealant materials including gelatin, chitosan, elastin, and pectin-based materials [15–19], there remains an urgent need for new sealants applicable to a broad range of lung injuries and diseases.

We therefore synthesized and screened a number of biologic materials [20], including those based on alginate, cellulose, chitosan, gelatin, and others and developed two potential candidate sealants, dopamine-conjugated alginate methacrylate (ALG-MA-DA) and dopamine-conjugated gelatin methacryloyl (GEL-MA-DA), that each have favorable viscoelastic and mechanical properties and demonstrated lack of cytotoxicity favorable for use on pleural and tracheal surfaces. Further, both performed well in *ex vivo* and *in vivo* pre-clinical pleural and tracheal injury models. Notably, the sealants take advantage of the adherence properties of mussel-inspired adherence proteins such as dopamine that are particularly effective for use on wet surfaces and as such, may offer advantages compared to those observed with gelatin methacryloyl and other comparable potential pleural sealants lacking dopamine conjugation [17]. As such, these are powerful new compounds for consideration in a range of clinical pulmonary applications.

## 2. Materials and methods

### 2.1. Base materials and methacrylation

Sodium alginate (Protanal, FMC Biopolymer) and gelatin (Sigma) were utilized as base materials. Methacrylation of alginate polymers was accomplished as previously described [19]. In brief, a 20-molar excess of methacrylic anhydride (Sigma) was added drop-wise to a 1% (w/v) sodium alginate solution over constant magnetic stirring at 600 rpm for the production of alginate methacrylate (ALG-MA). The reaction was allowed to proceed for 24 h, with the pH being regularly adjusted to 8 as needed via the addition of 5 N sodium hydroxide (NaOH, Fisher). The reaction vessel was maintained in an ice-bath during the reaction course. After 24 h of the reaction, the solution was transferred into a dialysis membrane (snakeskin 10 K molecular weight cut off, Thermo Fisher) and dialyzed for 7 days against deionized (DI) water with daily bath exchanges. The ALG-MA was then lyophilized prior to its downstream application or dopamine conjugation.

Gelatin methacryloyl (GEL-MA) was synthesized as previously described [19]. A 20% (w/v) solution of gelatin (porcine skin, 300 bloom strength, Sigma) was prepared in 0.25 M carbonate-bicarbonate buffer. The solution was adjusted to pH 9 using 5 N NaOH and placed on a magnetic stir plate set to 600 rpm and 50 °C. Methacrylic anhydride was added dropwise to the reaction vessel to achieve a final reaction ratio of 0.2 mL methacrylic anhydride per gram of dried gelatin. The reaction was allowed to proceed for 2 h prior to dilution with 5 vol of 1x phosphate-buffered saline (PBS) and pH adjustment to 7.4 by the drop-wise addition of 5 N NaOH. The GEL-MA was dialyzed against DI water with daily bath exchanges for 7 days prior to lyophilization and its downstream application or dopamine conjugation.

### 2.2. Dopamine conjugation

Dopamine conjugation to ALG-MA was accomplished using a carbodiimide-mediated reaction schema under nitrogen gas protection [20]. In brief, a 1% (w/v) ALG-MA solution was prepared from the lyophilized ALG-MA by dissolving in 50 mM 2-(N-morpholino)ethanesulfonic acid (MES, Sigma). This solution was reacted with 4 molar equivalents (relative to mannuronic acid's carboxyl groups) of

1-ethyl-3-(3-dimethylaminopropyl)carbodiimide hydrochloride (EDC, Sigma) and N-hydroxysuccinimide (NHS, Sigma). The reaction vessel was adjusted to a pH of 6 by the drop-wise addition of 1 N HCl and stirred for 45 min. Next, a 4 molar equivalent of dopamine hydrochloride (dopamine HCl, Sigma) was added to the reaction mixture. As the pH became quite low, the pH was brought back up to 4 by the drop-wise addition of 5 N NaOH for a total of 2 h. Finally, the reaction was adjusted to pH 6 by the drop-wise addition of 5 N NaOH for 12 h. The dopamine-conjugated alginate methacrylate (ALG-MA-DA) was then dialyzed against DI water with daily bath exchanges for 7 days prior to lyophilization. Final lyophilized compounds were stored under nitrogen gas at  $-20^{\circ}\text{C}$ .

The GEL-MA was similarly further modified with dopamine HCl with a carbodiimide-mediated reaction under nitrogen protection [20]. A 10% (w/v) solution of GEL-MA was prepared in 50 mM MES buffer and brought to  $50^{\circ}\text{C}$ . EDC and NHS were added to the reaction vessel at 0.15 M final concentrations and the pH of the reaction vessel was adjusted to 6 by the drop-wise addition of 1 N HCl. After 45 min, dopamine HCl was added to the reaction vessel to achieve a final concentration of 0.15 M. As the pH similarly became quite low, the pH was brought back up to 4 by the drop-wise addition of 5 N NaOH for 2 h, followed by a pH adjustment to 6 by the drop-wise addition of 5 N NaOH for a 12 hour reaction period. The dopamine-conjugated gelatin methacryloyl (GEL-MA-DA) was then dialyzed against DI water with daily bath exchanges for 7 days prior to lyophilization. Final lyophilized compounds were stored under nitrogen gas at  $-20^{\circ}\text{C}$ .

### 2.3. Photo-initiators and visible light crosslinking for liquid formulations

The respective ALG-MA, ALG-MA-DA, GEL-MA, or GEL-MA-DA solutions were mixed at  $37^{\circ}\text{C}$  in the dark with photo-initiator stock solutions such that the final concentration of the respective initiators was 0.00125% (w/v) for Eosin Y (Fisher), 125 mM for triethanolamine (Sigma), and 19 mM for 1-vinyl-2-pyrrolidinone (Sigma) [21,22]. Mixing was done in the dark to prevent premature curing. For photo-crosslinking liquid formulations of either ALG-MA-DA or GEL-MA-DA, either on the benchtop or after tissue application, the applied liquids were exposed to green light using light-emitting diodes (LEDs) of a wavelength of 525 nm (Super-bright LED) with visible cross-linking and solid patch formation occurring within five minutes for each compound. The photo-initiator stock solutions were stored protected from light at room temperature [22].

### 2.4. Photo-initiators and visible light crosslinking for patch formulations

Once each formulation was dissolved in nitrogen degassed DI water at 4% w/v, the photo-initiator cocktail was added to the solution in darkness. This solution was then injected into a custom-built Teflon mold of  $150\text{ mm} \times 150\text{ mm} \times 1\text{ mm}$  and frozen at  $-80^{\circ}\text{C}$  resulting in a 1 mm thick polymer sheet. The frozen polymer sheet was allowed to briefly thaw and was subsequently photo-crosslinked under green light emitting LEDs with solid patch formation occurring within 5 min before being refrozen at  $-80^{\circ}\text{C}$ . After discharging the polymer sheet from the mold, the sheet was lyophilized, and individual patches were prepared from the lyophilized sheet using a 6 mm diameter circular biopsy punch.

## 2.5. Chemical characterization

Materials were characterized using proton nuclear magnetic resonance ( $^1\text{H}$  NMR), and Fourier-Transform Infrared Spectrophotometry (FTIR), or gel-permeation chromatography (GPC) as appropriate. Each of the dried, methacryloyl precursors as well as the dopamine-conjugated materials was characterized with  $^1\text{H}$  NMR by Akina Inc. at Purdue University by the PINMRF group ([www.pinmrf.purdue.edu/](http://www.pinmrf.purdue.edu/)). GPC was performed on a Waters Breeze-2 system with 1 ml/min dichloromethane flow across three sequential GPC columns ( $7.6 \times 300$  mm, Phenomenex) and detected by refractive index. Molecular weight parameters were determined by comparison against polystyrene standards (Agilent PS2). FTIR was performed using either a cast film on KBr salt plate or by compression into a KBr pellet and scanned using a Nicolette Protégé 460 ESP FTIR spectrophotometer. Attempts at utilizing rheometry (TA instruments model AR550 rheometer) to determine molecular weight by dilute-polymer viscosity yielded unreliable results (data not shown).

## 2.6. Mechanical characterizations

**2.6.1. Shear rheometry**—The shear rheological behavior was studied using a DHR-3 rheometer (TA Instruments) with two parallel disks (50 mm diameter). This rheometer was preheated to a set temperature, 25 or 37 °C. After dissolving dried GEL-MA-DA without the initiator system in PBS to give 35% w/v at 40 °C, this solution was loaded to the lower disk. After lowering the upper disk to give the gap 1 mm, the sample edge was coated by Krytox™ general purpose oil 103 (DuPont) to avoid drying [22]. Once temperature was stabilized at the set temperature, oscillatory shear tests were performed. First, strain sweep tests were performed to map the linear regime in terms of strain. Then, using a fresh sample, frequency sweep tests were carried out within the linear regime. The magnitude of the complex viscosity *versus* frequency [22] was obtained.

**2.6.2. Tensile test**—The tensile strength of sealants was determined by a DHR-3 rheometer (TA Instruments) based on a modified method of the Standard Test Method for Strength Properties of Tissue Adhesives in Tension, ASTM F2258–05 [23] and the Standard Test Method for Tensile Properties of Plastics, ASTM D638–14 [24]. Each sample was cut to give strips of 20 mm  $\times$  5 mm with thickness between 0.5 and 1 mm prior to loading: Once each end of the strips was held by tensile fixtures of the DHR-3, the surface of the sample was coated by Krytox™ general purpose oil 103 (DuPont) to avoid drying [22]. The upper fixture was pulled at 6 mm/min at 20 °C until failure occurred, and the relevant force and strain were monitored. The tensile strength was obtained by the force value at failure by the cross-sectional area. Measurements were repeated 6 times with a fresh sample for each type of sealant. ALG-MA patches were used as is. ALG-MA-DA patches were oxidized by applying 10  $\mu\text{L}$  of the oxidant on top of patch for five minutes. Solutions of GEL-MA/photo-initiators/PBS or GEL-MA-DA/photo-initiators/oxidant/PBS at 35% w/v were cross-linked for five minutes by use of the green LED light.

**2.6.3. Lap-shear test**—The shear strength of sealants was determined by the DHR-3 based on the Standard Test Method for Strength Properties of Tissue Adhesives under Lap-Shear by Tension Loading, ASTM F2255–05 [25]. Patches of ALG-MA or ALG-MA-DA and solutions of GEL-MA or GEL-MA-DA were used. Collagen edible casing

(Lemproducts, OH, USA) sheets of substrate were soaked in 1X PBS for 1 hour at 20 °C and then cut into strips of 20 mm × 5 mm. A patch of ALG-MA or ALG-MA-DA was cut to be 10 mm × 5 mm and was applied on one end of one collagen strip. Then, 3 µL of the oxidizing solution was applied on top of the ALG-MA-DA strip, and another collagen strip was put on the sealant covering the whole area of the ALG-MA or ALG-MA-DA strip but leaving uncovered area of the first collagen strip exposed (overlapping area: 10 mm × 5 mm). On one end, where no sealant was applied, each collagen strip was held by tensile fixtures of the DHR-3. Five minutes after applying the oxidant on to the ALG-MA-DA and forming the three layers of ALG-MA and collagen strips, the upper fixture was pulled at 5 mm/min at 20 °C until failure occurred, and the relevant force and strain were monitored. The shear strength was obtained by the force value at failure by the overlapping area. Similarly, 50 µL solution of GEL-MA/photo-initiators/PBS or GEL-MA-DA/photo-initiators/oxidant/PBS at 35% w/v was applied on one end of one collagen strip to cover 10 mm × 5 mm giving 1 mm thickness of sealant. Another collagen strip was put on the sealant covering the whole area of the solutions of GEL-MA or GEL-MA-DA strip but leaving uncovered area of the first collagen strip exposed. This sample was held and tested by the tensile fixture as described above five minutes after applying the green LED light. Measurements were repeated with a fresh sample 6 times for each type of sealant.

**2.6.4. Peel test**—The peel strength of sealants was determined by the DHR-3 based on the Standard Test Method for Strength Properties of Tissue Adhesives in T-Peel by Tension Loading, ASTM F2256–05 [26]. Patches of ALG-MA or ALG-MA-DA and solutions of GEL-MA or GEL-MA-DA were used. Collagen edible casing (Lemproducts, OH, USA) sheets of substrate were soaked in 1X PBS for 1 hour at room temperature and then cut to be strips of 20 mm × 5 mm. A patch of ALG-MA or ALG-MA-DA was cut to be 10 mm × 5 mm and was applied on one end of one collagen strip. Then, 3 µL of the oxidizing solution was applied on top of the ALG-MA-DA strip, and another collagen strip was put on the sealant and first collagen strip covering the whole area of the ALG-MA-DA strip and the area with no sealant of the first collagen strip (overlapping area: 10 mm × 5 mm). One end of each collagen strip, where no sealant was applied, was held by tensile fixtures of the DHR-3. Five minutes after applying the oxidant and forming the three layers of ALG-MA and collagen strips, the upper fixture was pulled at 250 mm/min at room temperature until failure occurs, and the relevant force and strain were monitored. The peel strength was determined by the force at failure in Newton over the contact width in cm. Similarly, 50 µL solution of GEL-MA/photo-initiators/PBS or GEL-MA-DA/photo-initiators/oxidant/PBS at 35% w/v was applied on one end of one collagen strip to cover 10 mm × 5 mm giving 1 mm thickness of sealant. Another collagen strip was put on the sealant and first collagen strip covering the whole area of the sealant and the area with no sealant of the first collagen strip. This sample was held and tested by the tensile fixture as described above five minutes after applying the green LED light. Measurements were repeated 6 times with a fresh sample for each type of sealant.

**2.6.5. Burst pressure and adhesion testing**—Burst pressures were determined based on the Standard Test Method for Burst Strength of Surgical Sealants, ASTM F2392–04 [27] ( $N = 5$  per sealant). Patches of ALG-MA or ALG-MA-DA and solutions of GEL-

MA or GEL-MA-DA were used. Collagen edible casing (Lemproducts, OH, USA) sheets of substrate were soaked in 1X PBS for 1 hour at room temperature and cut with a metal machinist's punch to be disks with a diameter 25 mm. A circular defect of 3 mm diameter was created with a biopsy punch in the center of the circular collagen disk. After loading the collagen disk on the burst pressure device, ALG-MA or ALG-MA-DA were applied as patches of 15 mm diameter and 1 mm thickness over the circular defect on the collagen substrate. Five minutes after applying 10  $\mu$ L of the oxidant on top of the patches, testing started with air flow at 2 L/min while pressure and time were monitored. Like-wise, 177  $\mu$ L solution of GEL-MA/photo-initiators/PBS or GEL-MA-DA/photo-initiators/oxidant/PBS at 35% w/v was applied over the defect on the collagen disk. A 15 mm diameter circular Teflon Oring was placed around the sealant to ensure that sealant does not flow out of the diameter and to give uniform application, of 1 mm thickness. After a five-minute exposure to the green LED light to cross-link, air flow underneath the sealed defect was increased to 2 L/min while pressure and time were monitored until material failure. Measurements were repeated 5 times with a fresh sample for each type of sealant.

## 2.7. Cell viability

Potential toxicities of the sealants or their accompanying reagents (oxidizing agent, photo-initiator) were assessed on representative lung cells including: human bronchial epithelial cells (HBE-135-E6E7, CRL-2741, ATCC), human alveolar basal epithelial adenocarcinoma cells (A549, CCL-185, ATCC), human lung fibroblasts (HLF, CCD-19Lu, ATCC), and human pleural mesothelial cells (HPM, courtesy of Arti Shukla, University of Vermont, [28]). HBEs were cultivated in keratinocyte-serum free medium (Gibco) with 5 ng/mL human recombinant endothelial growth factor (EGF, Gibco), 0.05 mg/mL bovine pituitary extract (Gibco), 0.005 mg/mL insulin (Sigma), 500 ng/mL hydrocortisone (Sigma), and 1% Penicillin, Streptomycin (Gibco) and not used past passage 15. A549 cells were cultivated in modified Ham's F-12 K medium (Sigma) with 2 mM glutamine and 10% fetal bovine serum. HLFs were cultivated in Eagle's Minimum Essential Medium (Gibco), supplemented with 10% fetal bovine serum (FBS, Hyclone) and 100 IU/mL penicillin/100 mg/mL streptomycin (Corning) and not used past passage 10. HPMs were cultivated in 50:50 M199:MCDB106 medium (Invitrogen, Carlsbad, CA) supplemented with 15% FBS, 10 ng/mL EGF, 0.4  $\mu$ g/mL hydrocortisone, 50 units/mL penicillin and 100  $\mu$ g/mL streptomycin.

Cells were seeded in 96 well tissue culture plates (Corning) at a concentration of up to 10,000 cells per well, depending on cell type, in their respective culture media. After overnight incubation for attachment, cells were then incubated for 24 h with either 100  $\mu$ g of lyophilized polymerized (cross-linked) sealant, 100  $\mu$ g unpolymerized sealant, oxidizing agent (0.1% w/v sodium metaperiodate), or photo-initiator solution at the working concentrations described above. Cell viability was then assessed using resazurin dye (Alamar Blue, Thermo Scientific) as follows: [29] a resazurin stock was prepared by dissolving 1 g of dye in 100 mL sterile 1x PBS. This stock was diluted by mixing 60  $\mu$ L of the concentrated stock with 940  $\mu$ L of cell culture media creating a cell-specific working resazurin stock. Following 3 washes with 1x PBS, 90  $\mu$ L of cell media and 10  $\mu$ L of the working resazurin stock were added to each experimental well. Experimental blank wells were also prepared by adding 90  $\mu$ L media and 10  $\mu$ L working resazurin stock to cell

free wells. The 96 well plate was then protected from light and incubated for 3 h prior assessment using a fluorescent plate reader (BioTek, Winooski VT) at 530 nm excitation and 590 nm emission. After correction against the cell-free wells, cell viability was calculated as a percentage of live control wells that had been incubated with the resazurin dye but free of sealant or adjunct materials. Data were presented as an average of 5 experimental replicates per stimulation type from a single experiment.

## 2.8. Animal studies

Adult female (8–12 weeks) C57BL/6 mice were utilized for *ex vivo* studies. Adult female (8–12 weeks) Wistar or Sprague-Dawley rats (Charles River) were used for *in vivo* studies. Pig lungs were obtained from a local slaughterhouse and used for *ex vivo* studies. The University of Vermont and University of Connecticut Health Center Institutional Animal Care and Use Committees (IACUC) respectively approved all experimental work performed on animals in this study and all studies were carried out in strict accordance with institutional and AAALAC standards (UVM IACUC 16–003, UConn IACUC 101,225).

## 2.9. *Ex vivo* lung injury (mouse and pig)

The heart-lung-trachea bloc was removed from mice after euthanasia by intraperitoneal injection of sodium pentobarbital (150 mg/kg). These blocs were rinsed with sterile saline containing an antibiotic cocktail (500 IU/mL penicillin/500ug/mL streptomycin (5X pen/strep) (Lonza), 50 mg/L gentamicin (Cellgro), 2.5 ug/mL Amphotericin B (Cellgro) in 1X PBS solution), the trachea cannulated with a blunted 18 gage angiocatheter and connected to a small animal ventilator (Inspira ASV, Harvard Apparatus, Holliston MA) and ventilated with room air with 2.5 cc tidal volume (approximately 10 cc/kg body weight), respiratory rate 10 breaths/minute, and 5 cm H<sub>2</sub>O positive end expiratory pressure (PEEP).

Pig lungs were rinsed and perfused with sterile saline containing the antibiotic cocktail described above, the tracheas cannulated with a 5.5 mm endotracheal tube (Mallinckrodt, St. Louis MO) and the lungs ventilated at room air with 250 cc tidal volume for whole lungs (10 cc/kg body weight), 100 cc/kg for individual lobes, respiratory rate 10 breaths/minute, and 5 cm H<sub>2</sub>O PEEP (Pulmonetics LTV 1000, DRE, Louisville KY). Both rat and pig lungs were ventilated while immersed in a 37 °C heated saline bath. To induce injury, a puncture was made utilizing either an 18 g needle (rat) or 5 mm diameter biopsy punch (pig) inserted to a depth that resulted in air bubbling from the defect. Once persistent air leak was confirmed, ALG-MA-DA or GEL-MA-DA sealants were applied as either as an *in situ* formed hydrogel or as lyophilized pre-crosslinked hydrogel patches while continuously ventilating.

For liquid applications, while continuously ventilating, the defects were dabbed with sterile gauze to remove excess fluid and GEL-MA-DA applied utilizing a dual-lumen syringe (Medmix Systems) with GEL-MA-DA and photoinitiator solution (light protected) in one lumen and oxidant in the other with mixing of the respective solutions occurring during application. Application was performed over an approximate 10 s period using 0.2 ml in an approximate 0.5 cm circumference (rat) and 2 ml in an approximate 4–5 cm diameter (pig) around the wound. Photo-cross-linking was performed by immediate exposure to a custom built green light LED system (wavelength of 525 nm) until the sealants had adhered and



formed functional seals as indicated by cessation of visible bubble leaking, generally within 5 min of application.

For patch applications, while continuously ventilating, the defects were dabbed with sterile gauze to remove excess fluid and oxidant (0.1% w/v sodium metaperiodate, 0.1 ml in an approximate 0.5 cm circumference (mouse) and 1 ml in an approximate 4–5 cm diameter (pig) around the wound) pipetted onto the wound site followed immediately by application of the patch. As discussed above, oxidant was added to the patch application protocol to enhance polymerization of dopamine functional groups to enhance integrity as suggested by the literature and also to potentially enhance patch interaction with the underlying tissue [20,30].

## 2.10. *In vivo* lung injury studies (rat)

Following isoflurane anesthesia (1–4%) and endotracheal intubation of the rats with a blunted 18 gage angiocatheter (day 0), animals were ventilated with the Harvard Apparatus ventilator at tidal volume of 10cc/kg body weight, respiratory rate of 10 breaths/minute, and 5 cm H<sub>2</sub>O PEEP. Body temperature was maintained by keeping the animal on a heated 37 °C surface. The animals were then prepped and draped in standard sterile procedure using hair clippers to shave the chest and betadine sponges or Chloroprep sticks to sterilize skin. A thoracotomy incision was then performed at the level of the second nipple line, the chest wall muscles were separated using blunt dissection, and sharp dissection was used to incise the intercostal muscles of the 4th intercostal space in order to expose the right lung. A small self-retaining retractor was then inserted between the ribs and used to spread the ribs to obtain optimal exposure of the lung. A defect was created in the lung using an 18 gage needle inserted to a depth necessary to produce continuous visible air bubbling at the injury site. For ALG-MA-DA patch application, oxidant solution and then a 6 mm lyophilized patch were applied as described above. For GEL-MA-DA liquid application, GEL-MA-DA/photo-initiator solution and oxidant were applied utilizing a dual-lumen syringe with mixing of the respective solutions occurring during application as described above. Photo-cross-linking was performed by exposure to the LED system until the sealants had adhered formed functional patches as indicated by cessation of visible bubble leaking.

For short-term non-survival surgeries and screening of different sealant preparations, animals underwent euthanasia 2 h after injury and repair. Animals were assessed for gross repair of experimentally-induced leaks (*i.e.*, presence or absence of air bubbling).

For longer term survival surgeries, following satisfactory repair of the experimental injury (*ie.*, absence of air bubbling after sealant application), the thoracotomy was then repaired in three layers using 3–0 Vicryl or 4–0 Vicryl Rapide, first re-approximating ribs, then closing overlying muscle layer, and finally skin, all in a running fashion. The tracheal incision was closed with 3–0 Vicryl. Isoflurane anesthesia was discontinued and the animals were then extubated after spontaneous respirations resumed. Animals were observed daily for either one week or one month for any signs of respiratory or other distress or illness.

In one cohort of rats ( $n = 6$  for each sealant), animals were euthanized one week post-operatively by intraperitoneal (IP) administration of pentobarbital (150 mg/kg), the tracheas

cannulated with a blunted 18 gage angiocatheter via tracheal cut down, and animals ventilated with 100% nitrogen gas for several minutes to inflate lungs with nitrogen and allow for adequate rigor. The tracheas were then tied off with silk suture and chest CT scanning was performed to evaluate for evidence of pneumothorax. Following CT scanning, lung tissue at the site of injury and repair was excised for histologic analyses. In a parallel cohort of rats ( $n = 6$  for each sealant), animals were euthanized at one month with pentobarbital (150 mg/kg IP) followed by CT scanning, blood collection, and sampling of lung tissue for histologic analyses as described above.

### 2.11. *In vivo* tracheal injury studies (rats)

For initial studies, four adult (6–8 weeks) female Sprague-Dawley rats underwent general anesthesia with isoflurane and nosecone ventilation with 6–8 L/min O<sub>2</sub>. Two rats had a 0.2 cm laceration injury produced in the anterior trachea with a 15 scalpel blade; one underwent suture repair with 7–0 prolene and one had an ALG-MA-DA patch placed with oxidant added on top of the patch (0.5 cc/patch). The other two rats had an 18 gage needle puncture injury to the trachea, one underwent suture repair with 7–0 prolene and the other repair with an ALG-MA-DA patch. After muscle flap and skin closure, animals were disconnected from isoflurane and extubated upon spontaneous respiration. All 4 rats were observed daily and underwent euthanasia on post-operative day (POD) 14 and assessed for gross appearance of the tracheal wound site and repair, saline bubble leak testing, and histologic analyses of hematoxylin and eosin stained 5  $\mu$ m frozen tracheal sections.

In the next series of studies, twenty-five adult (6–8 weeks) female Sprague-Dawley rats underwent general anesthesia with isoflurane and nosecone ventilation with 6–8 L/min O<sub>2</sub>. In one group ( $n = 10$ ), a 3-cartilage length anterior tracheal laceration was produced using a 15 scalpel blade and an ALG-MA-DA patch placed over the defect with oxidant added on top of the patch (0.5 cc/patch). The control arm ( $n = 10$ ) underwent a 3-cartilage length tracheal laceration repaired with 7–0 prolene suture. One group ( $n = 5$ ) underwent a 3-cartilage length tracheal laceration which did not undergo any intervention at the injury site, and only had muscle flap and skin closure. All 5 of these rats showed signs of respiratory distress in the immediate postoperative period, and died by postoperative day 1. All rats subsequently underwent euthanasia on POD14 and were assessed for gross appearance of the tracheal wound site and repair, saline bubble leak testing, and histologic analyses of hematoxylin and eosin stained 5  $\mu$ m frozen tracheal sections. Saline burst pressure was also tested *ex vivo* by removing the three tracheas each from the patch and suture repair groups, respectively, postmortem and cannulating each end with a 14 gage catheter with the proximal end connected to a syringe and the distal end tightly secured to a manometer. The pressure at which injury site burst was recorded for each specimen as saline was delivered via syringe into specimen.

### 2.12. Histologic assessments

Sections of the lung or trachea around the repaired wounds (approximately  $1 \times 1 \text{ cm}^3$ ) were excised and frozen in OCT (Tissue-Tek; Sakura Finetek USA). No inflation pressure was utilized during the fixation in order to not alter the adhesion of the patch to the injured lung or trachea. Hematoxylin and eosin stained 5  $\mu$ m thick frozen sections were assessed

by bright field light microscopy. Of note, initial attempts at paraformaldehyde fixation and paraffin embedding were determined to be unsuitable due to any residual sealant being washed out by the alcohols and xylenes utilized during de-parafinization.

### 2.13. Statistical analyses

Differences in mechanical properties before and after dopamine conjugation were analyzed with unpaired Student's *t*-test. Cytotoxicity analysis of each cell type was performed using one way ANOVA. All data are represented as percent of control (cells cultured in tissue culture plastic at the same time point)  $\pm$  standard deviation. Post-analysis multiple comparisons were conducted using the Tukey test with a 95% confidence level. All statistical analyses were performed using GraphPad Prism 6. *p* values  $\leq 0.05$  were considered statistically significant.

## 3. Results

A wide range of biologic compounds, functionalization, and cross-linking strategies were initially evaluated utilizing ASTM burst pressure testing as a screening modality. These identified alginate methacrylate (ALG-MA) and gelatin methacryloyl (GEL-MA) as promising initial parent compounds with dopamine conjugation improving the adhesive properties in both. Synthetic pathways of dopamine-conjugated alginate methacrylate (ALG-MA-DA) and dopamine-conjugated gelatin methacryloyl (GEL-MA-DA) are depicted in Fig. 1. Representative NMR spectra depict characteristic peaks for methacryl and dopamine groups for each material shows that methacryl groups were added successfully in all modified materials, and dopamine groups were successfully conjugated to ALG-MA-DA and GEL-MA-DA (Fig. 2). The quantification of each group was not performed since that is beyond the scope of this study. However, these demonstrate that alginate derivatives have the degree of dopamine conjugation well higher than that of methacryl group. Gelatin derivatives show the opposite behavior. Fig. 3 shows the magnitude of the complex viscosity *versus* frequency for 35% w/v solution of GEL-MA-DA/DI water at 25 and 37 °C. The magnitude at 25 °C is  $10^3$  to  $10^6$  higher than that at 37 °C. Gelatin derivatives go through sol-gel (physical gelation) transition below 30 °C [22] while alginate derivatives do not, and thus understanding the flow property of GEL-MA-DA is important for applications.

Mechanical testing was then performed on ALG-MA-DA and GEL-MA-DA, comparing both to each other and to ALG-MA and GEL-MA, respectively. Notably, the ALG-MA-DA hydrogel formulation tended to gel quickly while being applied with a dual lumen syringe, comparable to what occurs during clinical use of ProGel™ [13]. Conversely, the GEL-MA-DA hydrogel formulation was easily applied without clogging of the dual lumen application syringe. Both ALG-MA-DA and GEL-MA-DA were easily formulated into pre-formed patches. Both ALG-MA-DA and GEL-MA-DA demonstrated enhanced tensile, shear, and peel strengths compared to their non-conjugated counterparts (Fig. 4a–c). Dopamine conjugation enhanced burst pressure performance of both ALG-MA and GEL-MA with values 16 times higher in ALG-MA-DA compared to ALG-MA, although with higher variance in ALG-MA-DA, and 3 times higher in GEL-MA-DA compared to

GEL-MA (Fig. 4d). Notably, the recorded burst pressure of 250 cm H<sub>2</sub>O surpasses the 218 cm H<sub>2</sub>O burst pressure reported for Progel™ [14].

Neither ALG-MA-DA nor GEL-MA-DA demonstrated obvious toxic effects on growth of a range of relevant lung cell types including human lung airway epithelial (HBE), alveolar carcinoma (A549), human lung fibroblast (HLF), and human pleural mesothelial cells (HPM) (Fig. 5a). This include both photo-cross-linked (polymerized) as well as non-polymerized compounds despite significant effects on cell viability observed with the photo-initiator cocktail or oxidant alone, particular with HBE, HLF and HPM cells (Fig. 5b). This demonstrates that although the photo-initiator compounds or oxidants utilized can be toxic toxicity is removed as the compounds are used up or washed out.

To initially screen sealant adherence to lung tissue, *ex vivo* models of isolated ventilated rat and pig lungs were utilized (Fig. 6). Qualitatively, no air leaks were observed after sealant application onto experimentally-induced defects allowing full inflation and ventilation of the lungs. Initially both ALG-MA-DA and GEL-MA-DA were assessed in both *in situ* formed hydrogel and pre-formed hydrogel patch formulations. However, as described above, ALG-MA-DA *in situ* formed hydrogel application was hindered by gel formation occurring rapidly with mixing in the dual lumen syringes whereas, despite robust burst pressure and peel testing results, the GEL-MA-DA patch formulation was less adherent than the ALG-MA-DA patch formulation. These observations were confirmed in short term (2 hr) non-survival *in vivo* studies in rats (data not shown). As such, further long-term *in vivo* studies were conducted in rats utilizing either ALG-MA-DA patch or GEL-MA-DA *in situ* formed hydrogel applications (Fig. 7a–c). Assessing rats either 1 week (ALG-MA-DA *n* = 3, GEL-MA-DA, *n* = 6) or 1 month (ALG-MA-DA *n* = 6, GEL-MA-DA, *n* = 6) after injury and sealant application demonstrated good adherence of the sealants both grossly (Fig. 7d–f) and histologically and no obvious air leak or pneumothorax by fluoroscopy or CT scanning (2 each of 1 week and 1 month ALG-MA-DA and GEL-MA-DA animals had what were felt to be small iatrogenic pneumothoraces at euthanasia). Histologic analyses demonstrated juxtaposition of the sealant with underlying lung tissue with no obvious inflammatory cell infiltrates in hematoxylin and eosin stained sections (Fig. 8). Residual sealant was observed in 1 week GEL-MA-DA-treated animals and in both 1 week and 1 month ALG-MA-DA-treated animals.

We further assessed whether ALG-MA-DA patches would be potentially also applicable to tracheal injuries. Using an *in vivo* rat model of tracheal injury induced with scalpel laceration, ALG-MA-DA was easily applied and formed a durable seal, comparable to suture repair, as assessed over a two week period (Error! Reference source not found.) Burst pressure testing on isolated 3 rat tracheas harvested from patch and suture repair groups, respectively, demonstrated comparable strength to that provided with conventional sutures (Fig. 9a,b). Gross and histologic analyses demonstrated juxtaposition of the sealant with underlying lung tissue with no obvious inflammatory cell infiltrates (Fig. 9c–f).

## 4. Discussion

Current treatments for persistent pleural and tracheobronchial injuries require prolonged chest tube drainage (pleural) and/or invasive surgery (both) with associated high morbidity and costs. One way to repair these injuries is with the use of a sealant, ideally, one that is simple to apply and that adheres and seals quickly. In addition, a sealant that allows for normal growth and development over time would enable use in neonatal and pediatric populations with congenital tracheobronchial defects, currently a significant unmet need. While the concept of developing a pleural/tracheal sealant is itself not novel, no compounds evaluated to date have proven long term success. This includes a range of materials such as fibrin, cyanoacrylates, and others, often described in individual case reports or small case series [6–12,31–33]. Progel TM (Bard-Davol Inc.) is the only FDA-approved pleural sealant in the US. However, it is only approved for use in open surgical pulmonary resections and not for other lung injuries or for tracheal injuries including traumatic injuries. Recent studies with chitosan, pectin, and elastin-based compounds have shown promise in pre-clinical lung injury models [15–17] but there remains an urgent need for new sealants applicable to a broad range of lung and tracheobronchial injuries and diseases.

Natural based biomaterials can be advantageous compared to their synthetic counterparts due to heightened compatibility and less potential inflammatory or immune response. Recent reports investigating plant-derived pectin or methacrylated elastin suggest that a range of previously unexplored biomaterials may also have appropriate attributes for use as pleural sealants. Alginate and alginate-based hydrogels are increasingly investigated for biomedical applications due to their inherent non-toxicity, biocompatibility, and availability [18,34–39]. Derived from brown algae, alginate is desirable not only for those attributes already listed, but also for its relatively low cost and the various applications it can be used for drug delivery and tissue engineering. Comparably, low cost gelatin and gelatin-based hydrogels can be derived from several mammalian sources including porcine and bovine tissues and are widely used in food, pharmaceutical, and other medical applications [19]. Functionalization of both alginate and gelatin with controlled methacrylation has been described to enhance physical attributes advantageous for potential use as lung sealants [18,39]. Methacrylation further imparts a functional group capable of light-activated covalent crosslinking by free radical polymerization in the presence of a photo-initiator for example Eosin Y using either visible or mono-spectrum light, advantageous compared to crosslinking with UV light spectra [21]. In parallel, L-dopa, the major adhesive functional group in mussel-foot proteins which particularly increases adherence in moist/wet conditions that characterize pleural and tracheobronchial surfaces is increasingly recognized as a powerful adhesive with a number of potential biomedical applications [20,30,40,41]. A dopamine-conjugated gelatin methacryloyl compound has recently been reported and proposed for use in biomedical applications [42].

Materials with dual functionality offer the adhesivity of catechol groups along with the mechanical bolstering and visible light polymerizing ability of methacrylate groups. Combining these functionalizations with both alginate and gelatin, we have demonstrated simple low-cost synthetic approaches producing two materials, ALG-MA-DA and GEL-MA-DA, each with desirable mechanical and materials properties as well as absence of

significant degradation and lack of obvious cell toxicity. Notably, burst pressure and other mechanical profiling compares favorably with ProGel™ and with other new sealant compounds recently evaluated [13,15–17]. The gelatin concentration of 25% w/v utilized was based on previously published work [43] and alginate concentrations of 4% investigated as this was the highest concentration that most readily flowed into the mold utilized for patch formation. Similarly, 5 min photo-activation cross-linking time was based on previous experience [18] and was effective in the *ex vivo* and *in vivo* models. Importantly this included successful use on wet surfaces during both mechanical and *in vivo* testing, for example lap shear and peel testing in which the materials substrates were soaked in PBS prior to actual testing. In addition, the surfaces of the lungs in both the *ex vivo* and *in vivo* testing were moist. As such, the sealant materials were both quantitatively and qualitatively demonstrated to work on wet surfaces. While these are effective initial working parameters and provide proof of concept support for use of the ALG-MA-DA pre-formed hydrogel patch and GEL-MA-DA *in situ* formed hydrogel liquid for pleural and tracheal injuries, further studies may reveal other effective formulations, including use of ALG-MA-DA *in situ* formed hydrogel form, and further reduction in cross-linking time. We are also not clear as to why dopamine conjugation affected tensile strength though dopamine-dopamine mediated polymer chain crosslinking and alterations in hydrogen bonding are suspected. As such, future studies will more fully characterize the chemical aspects of the ALG-MA-DA and GEL-MA-DA compounds including rates of substitution and optimization of methacryl and dopamine conjugation as well as more fully investigate rheological properties including effects of polymer and photo-initiator concentrations on cross-linking kinetics. Degradation and swelling studies will also be performed with more optimized formulations.

Initial testing had also included ALG-MA-DA *in situ* formed hydrogel and GEL-MA-DA pre-formed hydrogel patch formulations. However, ALG-MA-DA *in situ* formed hydrogel application was hindered by rapid gel formation when mixed with the oxidant in the dual lumen syringes utilized for tissue application whereas the GEL-MA-DA patch formulation was less adherent to lung tissue than the ALG-MA-DA patch formulation. As such, further rheological, mechanical, and biologic assessments were focused on patches of ALG-MA and ALG-MA-DA and solutions of GEL-MA or GEL-MA-DA and will be further directly compared to ProGel™ in parallel studies.

Both ALG-MA-DA and GEL-MA-DA performed well in *ex vivo* rat and pig lung injury models and *in vivo* models of rat lung and tracheal injuries for up to one month and two weeks, the longest times evaluated to date, respectively. No obvious gross or histologic toxicities were observed including no evidence of sealant-induced tissue inflammation. This opens up a range of application possibilities using both direct patch application in the operating room or to open trauma wounds as well use *in situ* formed hydrogel application either directly or through thoroscopic or even bronchoscopic administration.

The initial success of these compounds is promising in the current proof of concept studies and ongoing investigations will evaluate them further in adult pig models of lung and tracheal injuries and also in models of pediatric tracheal injury to assess potential efficacy in support of long-term tracheal growth and thus applicability to congenital tracheal defects. These studies will also further assess the chemical and mechanical characteristics of the

sealant materials as well as assess any potential serum or systemic toxicities associated with use of either sealant. We have to date included an oxidant with use of the dopamine-conjugated materials as the available literature suggests that this will enhance dopamine crosslinking. However, further refinements may also remove need for an oxidant and further simply use of both ALG-MA-DA and GEL-MA-DA applications. Information gathered from use of sealant materials in other organs such as intestines may also provide useful in further refinements [44,45].

## 5. Conclusions

New easy-to-use pleural and tracheobronchial tree sealants will offer important new treatment approaches for a range of pleural and tracheal including both non-military and military (battlefield trauma). Two new compounds, ALG-MA-DA and GEL-MA-DA have favorable materials properties and have performed well in initial *ex vivo* lung injury models and *in vivo* small animal models of pleural and tracheal injuries. Further studies will further characterize and refine the sealant compounds and further evaluate utility in larger animal models as a prelude to potential clinical investigations.

## Acknowledgments

The authors gratefully acknowledge Loredana Asarian and Alicia Tanneberger for technical assistance, Arti Shukla PhD and Keith Monsen for the human pleural mesothelial cells, the staffs of the UVM and UConn animal care facilities, and Spencer Fenn and Darcy Wagner for assistance with *ex vivo* mouse lung studies.

## Funding

Dr. Weiss was supported by SPARK funding from the University of Vermont and by Department of Defense (USA) PRMRP Medical Discovery Award W81XWH-15-1-0107. Dr. Finck was supported by the Peter Deckers Endowed Chair at the Connecticut Children's Medical Center (USA). Dr. Park was supported by Department of Chemical and Process Engineering, University of Canterbury (New Zealand).

## References

- [1]. 2008 Medicare De-Identified Database. [https://www.cms.gov/Research-Statistics-Data-and-Systems/Statistics-Trends-and-Reports/BSAPUFS/index.html?redirect=/BSAPUFS/03\\_Inpatient\\_Claims.asp](https://www.cms.gov/Research-Statistics-Data-and-Systems/Statistics-Trends-and-Reports/BSAPUFS/index.html?redirect=/BSAPUFS/03_Inpatient_Claims.asp).
- [2]. [http://www.health.mil/~media/MHS/Presentation%20Files/Eastridge\\_DHB%20Death%20on%20the%20Battlefield%20Final.ashx](http://www.health.mil/~media/MHS/Presentation%20Files/Eastridge_DHB%20Death%20on%20the%20Battlefield%20Final.ashx).
- [3]. Lanigan A, Lindsey B, Maturo S, Brennan J, Laury A, The Joint Facial and Invasive Neck Trauma (J-FAINT) project, Iraq and Afghanistan: 2011–2016, *Otolaryngol. Head Neck Surg.* 157 (4) (2017 Oct) 602–607 Epub 2017 Aug 22. doi: 10.1177/0194599817725713.
- [4]. Porte HL, Jany T, Akkad R, Conti M, Gillet PA, Guidat A, et al. , Randomized controlled trial of a synthetic sealant for preventing alveolar air leaks after lobectomy, *Ann. Thorac. Surg* 71 (2001) 1618–1622. [PubMed: 11383810]
- [5]. Wain JC, Kaiser LR, Johnstone DW, Yang SC, Wright CD, Friedberg JS, et al. , Trial of a novel synthetic sealant in preventing air leaks after lung resection, *Ann. Thorac. Surg* 71 (2001) 1623–1629. [PubMed: 11383811]
- [6]. Health FaDACfDaR. Summary of Safety and Effectiveness Data (for FocalSeal-L Synthetic Absorbable Sealant). 2000.
- [7]. Dango S, Lin R, Hennings E, Passlick B, Initial experience with a synthetic sealant PleuraSealTM after pulmonary resections: a prospective study with retrospective case matched controls, *J. Cardiothorac. Surg* 5 (2021) 52010.

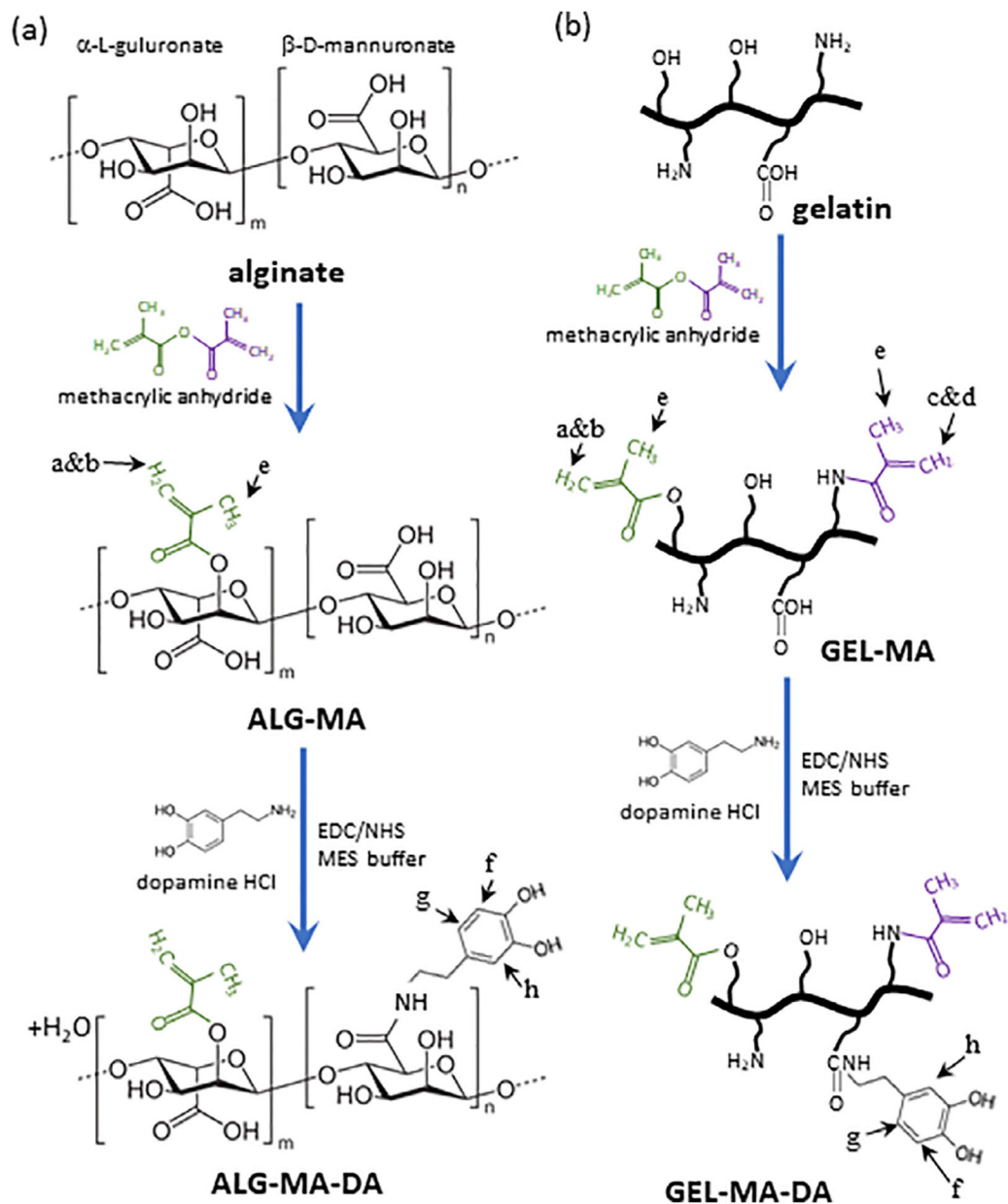
- [8]. Fabian T, Federico JA, Ponn RB, Fibrin glue in pulmonary resection: a prospective, randomized, blinded study, *Ann. Thorac. Surg* 75 (2003) 1587–1592. [PubMed: 12735583]
- [9]. Allen MS, Wood DE, Hawkinson RW, Harpole DH, McKenna RJ, Walsh GL, Vallieres E, Miller DL, Nichols FC 3rd, Smythe WR, Davis RD, 3 M Surgical Sealant Study Group Prospective randomized study evaluating a biodegradable polymeric sealant for sealing intraoperative air leaks that occur during pulmonary resection, *Ann. Thorac. Surg* 77 (2004) 1792–1801. [PubMed: 15111188]
- [10]. Schneider T, Storz K, Dienemann H, Hoffmann H, Management of iatrogenic tracheobronchial injuries: a retrospective analysis of 29 cases, *Ann. Thorac. Surg* 83 (2007) 1960–1964. [PubMed: 17532378]
- [11]. Grillo HC, Development of tracheal surgery: a historical review. Part 2.: treatment of tracheal diseases, *Ann. Thorac. Surg* 75 (2003) 1039–1047. [PubMed: 12645751]
- [12]. Cerezal-Garrido LJ, Agudo-Bernal J, Vaquero-Puerta C, Histological benefits of sealants in tracheal lesions in wistar rats, *Surg. Technol. Int* (2016 Apr 28) 29–35.
- [13]. Fuller C, Reduction of intraoperative air leaks with Progel in pulmonary resection: a comprehensive review, *J. Cardiothorac. Surg* 8 (2013) 90–97. [PubMed: 23590942]
- [14]. Progel Pleural Air Leak Sealant Value Analysis Committee Product Information Kit. Bard Davol, Inc. <http://www.davol.com/default/assets/File/Progel%20VAC%20Brochure.pdf>.
- [15]. Fernandez JG, Seetharam S, Ding C, Feliz J, Ingber DE Doherty, Direct bonding of chitosan biomaterials to tissues using transglutaminase for surgical repair or device implantation, *Tissue Eng. Part A* 23 (2017) 135–142. [PubMed: 27869543]
- [16]. Annabi N, Zhang YN, Assmann A, Sani ES, Cheng G, Lassaletta AD, Vegh A, Dehghani B, Ruiz-Esparza GU, Wang X, Gangadharan S, Weiss AS, Khademhosseini A, Engineering a highly elastic human protein-based sealant for surgical applications, *Sci. Transl. Med* 9 (410) (2017 Oct 4) pii: eaai7466, doi: 10.1126/scitranslmed.aai7466. [PubMed: 28978753]
- [17]. Servais AB, Valenzuela CD, Kienzle A, Ysasi AB, Wagner WL, Tsuda A, Ackermann M, Mentzer SJ, Functional mechanics of a pectin-based pleural sealant after lung injury, *Tissue Eng. Part A* 24 (9–10) (2018 May) 695–702 Epub 2018 Jan 5., doi: 10.1089/ten.tea.2017.0299. [PubMed: 28920559]
- [18]. Wagner DE, Fenn SL, Bonenfant NR, Marks ER, Borg Z, Saunders P, Oldinski RA, Weiss DJ, Design and synthesis of an artificial pulmonary pleura for high throughput studies in acellular human lungs, *Cell. Mol. Bioeng* (2014) 1–12. [PubMed: 24563678]
- [19]. Garner J, Park K, Chemically modified natural polysaccharides to form gels, *Polysaccharides* (2015) 1555–1582.
- [20]. Wei Q, Zhang Z, Li J, Li B, Zhao C, Oxidant-induced dopamine polymerization for multifunctional coatings, *Polym. Chem* 2010 (1) (2010) 1430–1433.
- [21]. Lilly JL, Gottipati A, Cahall CF, Agoub M, Berron BJ, Comparison of eosin and fluorescein conjugates for the photoinitiation of cell-compatible polymer coatings, *PLoS ONE* 13 (1) (2018 Jan 8) e0190880 eCollection 2018. doi: 10.1371/journal.pone.0190880. [PubMed: 29309430]
- [22]. Park HE, Gasek N, Hwang J, Weiss DJ, Lee PC, Effect of temperature on gelation and cross-linking of gelatin methacryloyl for biomedical applications, *Phys. Fluids* 32 (2020) 3, doi: 10.1063/1.5144896.
- [23]. ASTM F2258–05(2015) Standard Test Method for Strength Properties of Tissue Adhesives in Tension. Book of Standards Volume: 13.01.
- [24]. ASTM D638–14 Standard Test Method for Tensile Properties of Plastics. Book of Standards Volume: 08.01 2021
- [25]. ASTM F2255–05(2015) Standard Test Method for Strength Properties of Tissue Adhesives in Lap-Shear by Tension Loading. Book of Standards Volume: 13.01.
- [26]. ASTM F2256–05 (2015) Standard Test Method for Strength Properties of Tissue Adhesives in T-Peel by Tension Loading. Book of Standards Volume: 13.01.
- [27]. ASTM-F2392–04 Standard Test Method for Burst Strength of Surgical Sealants Annu. Book ASTM Stand. 2015



- [28]. Dragon JI, Thompson J2, MacPherson M2, Shukla A, Differential susceptibility of human pleural and peritoneal mesothelial cells to asbestos exposure, *J. Cell. Biochem* 116 (8) (2015 Aug) 1540–1552. [PubMed: 25757056]
- [29]. Ren X, Moser PT, Gilpin SE, Okamoto T, Wu T, Tapias LF, Mercier FE, Xiong L, Ghawi R, Scadden DT, Mathisen DJ, Ott HC, Engineering pulmonary vasculature in decellularized rat and human lungs, *Nat. Biotechnol* 33 (10) (2015 Oct) 1097–1102. [PubMed: 26368048]
- [30]. Scognamiglio F, Travan A, Borgogna M, Donati I, Marsich E, Bosmans JW, Perge L, Foulc MP, Bouvy ND, Paoletti S, Enhanced bioadhesivity of dopamine-functionalized polysaccharidic membranes for general surgery applications, *Acta Biomater.* 44 (2016 Oct 15) 232–242, doi: 10.1016/j.actbio.2016.08.017. [PubMed: 27542316]
- [31]. Chen WH, Chu Y, Wu YC, Liu CY, Yuan HC, Ko PJ, Liu YH, Endoscopic closure of a tracheal access site using bioglue after transtracheal thoracoscopy in a non-survival canine surgery model, *Eur. Surg. Res* 48 (2012) 26–33. [PubMed: 22189409]
- [32]. Liu YH, Liu HP, Wu YC, Ko PJ, Secure closure of the tracheal incision after natural orifice transluminal endoscopic surgery with a surgical sealant (CoSeal), *Surg. Innov* 18 (2011) N7–N8.
- [33]. Huei TJ, Lip HTC, Rahmat O, Major tracheobronchial injuries: management of two rare cases, *Med. J. Malaysia* 73 (3) (June 2018).
- [34]. Lee KY, Mooney DJ, Alginate: properties and biomedical applications, *Prog. Polym. Sci* 37 (2012) 106–126. [PubMed: 22125349]
- [35]. Pawar SN, Edgar KJ, Alginate derivatization: a review of chemistry, properties and applications, *Biomaterials* 33 (2012) 3279–3305. [PubMed: 22281421]
- [36]. Moller L, Krause A, Dahlmann J, Gruh I, Kirschning A, Drager G, Preparation and evaluation of hydrogel-composites from methacrylated hyaluronic acid, alginate, and gelatin for tissue engineering, *Int. J. Artif. Organs* 34 (2011) 93–102. [PubMed: 21374568]
- [37]. Bouhadir KH, Lee KY, Alsberg E, Damm KL, Anderson KW, Mooney DJ, Degradation and partially oxidized alginate and its potential application for tissue engineering, *BiotechProgress* 17 (2001) 945–950.
- [38]. Teixeira LS, Feijen J, van Blitterswijk CA, Dijkstra PJ, Karperien M, Enzyme-catalyzed crosslinkable hydrogels: emerging strategies for tissue engineering, *Biomaterials* 33 (5) (2012 Feb) 1281–1290, doi: 10.1016/j.biomaterials.2011.10.067. [PubMed: 22118821]
- [39]. Charron PN, Fenn SL, Poniz A, Oldinski RA, Mechanical properties and failure analysis of visible light crosslinked alginate-based tissue sealants, *J. Mech. Behav. Biomed. Mater* 59 (2016 Jun) 314–321. [PubMed: 26897093]
- [40]. Qin Z, Buehler MJ, Molecular mechanics of mussel adhesion proteins, *J Mech. Phys. Solid* 62 (2014) 19–30.
- [41]. Ma H, Luo J, Sun Z, Xia L, Shi M, Liu M, Chang J, Wu C, 3D printing of biomaterials with mussel-inspired nanostructures for tumor therapy and tissue regeneration, *Biomaterials* 111 (2016 Dec) 138–148 Epub 2016 Oct 5. doi: 10.1016/j.biomaterials.2016.10.005. [PubMed: 27728813]
- [42]. Kim JY, Ryu SB, Park KD, Preparation and characterization of dual-crosslinked gelatin hydrogel via Dopa-Fe<sup>3+</sup> + complexation and fenton reaction, *J Industrial and Engineering Chemistry* 58 (2018) 1-5-112.
- [43]. Assmann A, Vegh A, Ghasemi-Rad M, Bagherifard S, Cheng G, Sani ES, Ruiz-Esparza GU, Noshadi I, Lassaletta AD, Gangadharan S, Tamayol A, Khademhosseini A, Annabi N, A highly adhesive and naturally derived sealant, *Biomaterials* 140 (2017) 115–127. [PubMed: 28646685]
- [44]. Hong S, Priovich D, Kilcoyne A, Huang CH, lee H, Weissleder R, Supramolecular metallo-bioadhesive for minimally invasive use, *Adv. Mater* 28 (2016) 8675–8680. [PubMed: 27515068]
- [45]. Ryu JH, Kim HJ, Kim K, Yoon GS, Wang Y, Choi GS, Lee H, Park JS, Multipurpose intraperitoneal adhesive patches, *Adv. Funct. Mater* 29 (2019) 1900495.

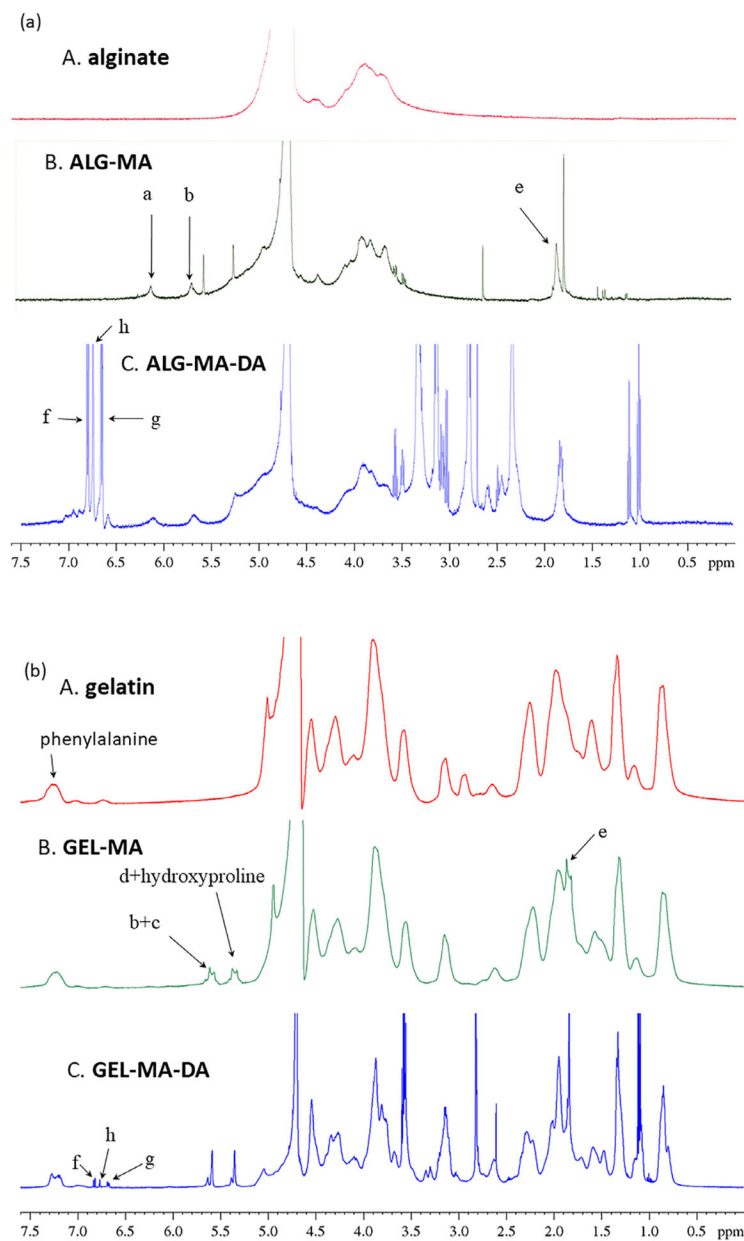
### Statement of significance

Pneumothorax and pleural effusions resulting from trauma and a range of lung diseases and critical illnesses can result in lung collapse that can be immediately life-threatening or result in chronic leaking (bronchopleural fistula) that is currently difficult to manage. This leads to significantly increased morbidity, mortality, hospital stays, health care costs, and other complications. We have developed sealants originating from alginate and gelatin biomaterials, each functionalized by methacryloylation and by dopamine conjugation to have desired mechanical characteristics for use in pleural and tracheal injuries. The sealants are easily applied, non-cytotoxic, and perform well *in vitro* and *in vivo* model systems of lung and tracheal injuries. These initial proof of concept investigations provide a platform for further studies.



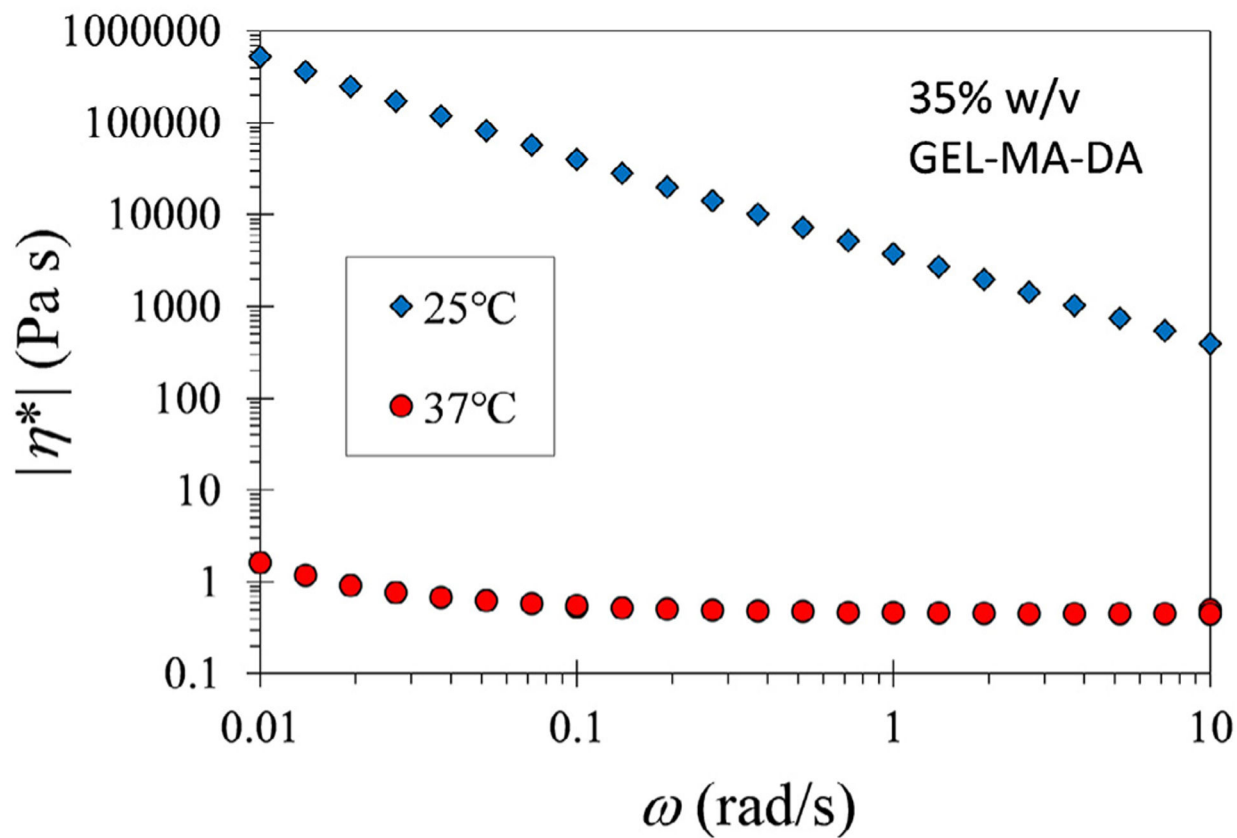
**Fig. 1. Scheme for chemical modification to prepare dopamine conjugated sealants.**

(a) Alginate derivatives. (b) Gelatin derivatives. Two different methacryl groups can be formed: methacrylamide (purple) and methacrylate (green). Letter a through f designate NMR peak assignments. EDC = 1-ethyl-3-(3-dimethylaminopropyl)carbodiimide hydrochloride, NHS = *N*-hydroxysuccinimide.



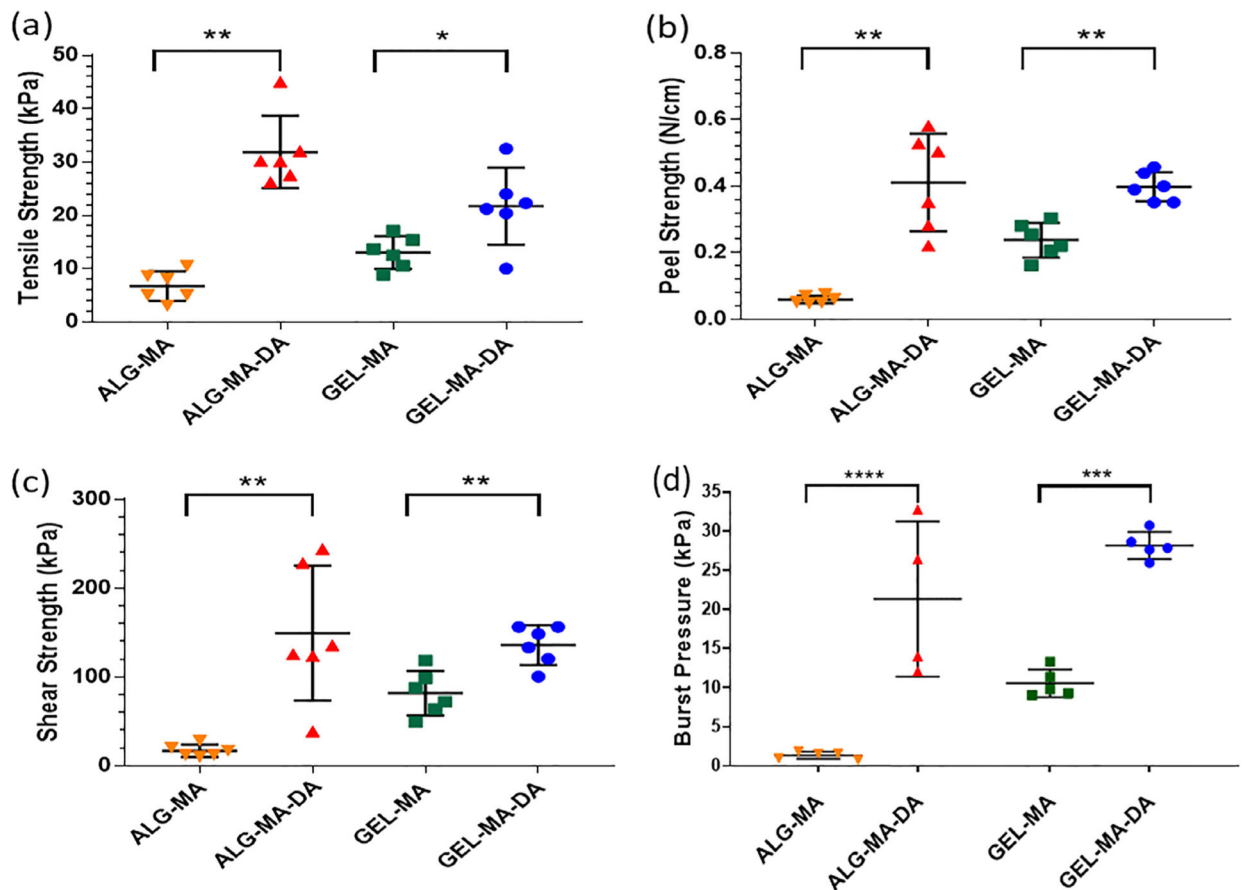
**Fig. 2. NMR spectra of the sealant materials.**

(a) Alginate derivatives: sodium alginate (A), ALG-MA (B), and ALG-MA-DA (C). Methacryl group addition was confirmed via peaks (a, b, and e in Fig. 1) in both ALG-MA and ALG-MA-DA. (b) Gelatin derivatives: gelatin (A), GEL-MA (B), and GEL-MA-DA (C). Methacryl group addition was confirmed via peaks (a through e in Fig. 1) in both GEL-MA and GEL-MA-DA. Dopamine conjugation was confirmed via peaks (f through g in Fig. 1) of the aromatic protons between 6.6 and 7 ppm in both ALG-MA-DA and GEL-MA-DA. All chemical shifts relative to D<sub>2</sub>O tuning.



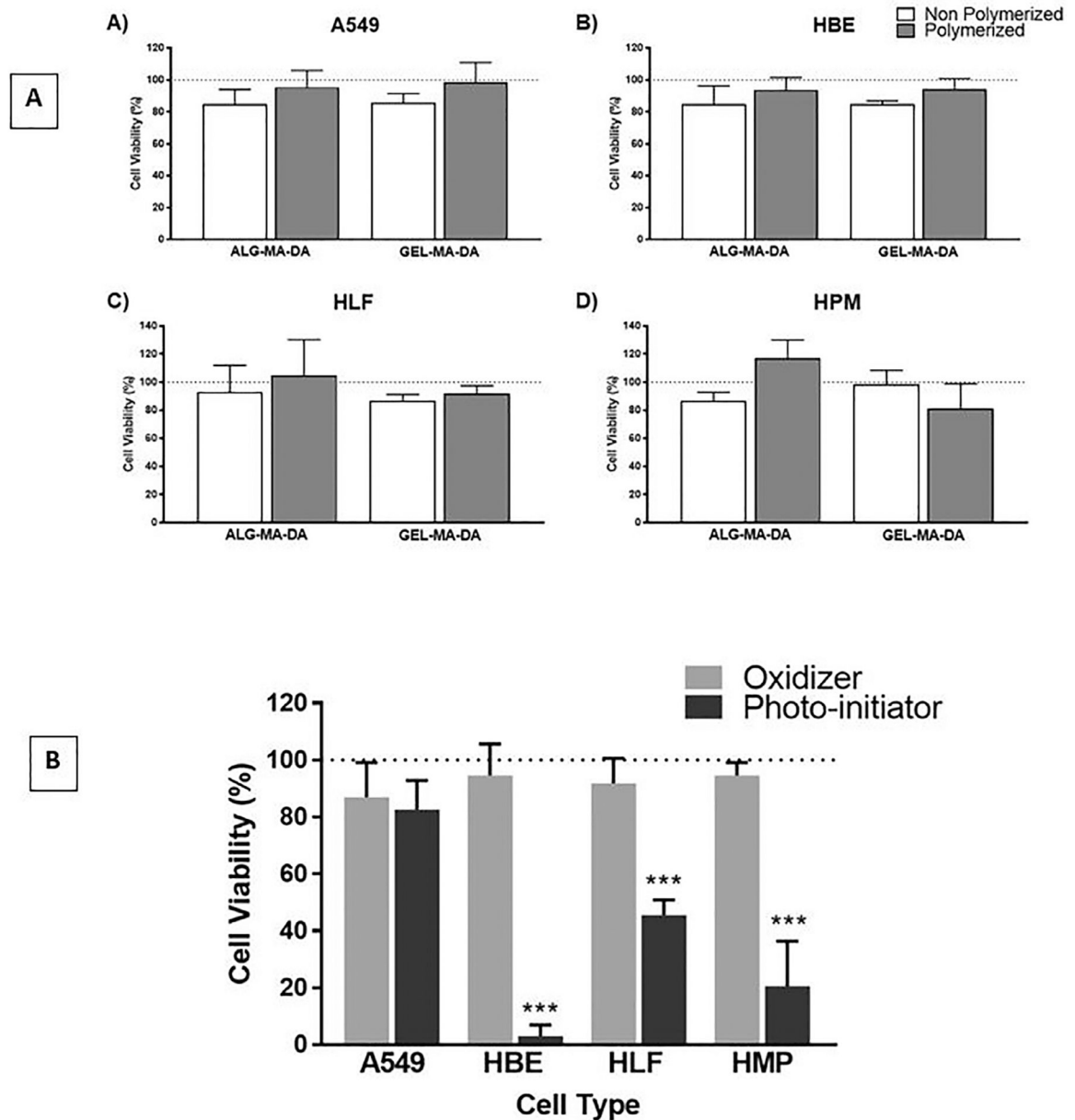
**Fig. 3. Shear rheometry.**

The magnitude of complex viscosity *versus* frequency for 35% w/v solution of GEL-MA-DA/DI water at 25 and 37 °C. The magnitude at 25 °C is significantly higher than that at 37 °C due to physical gelation [22].

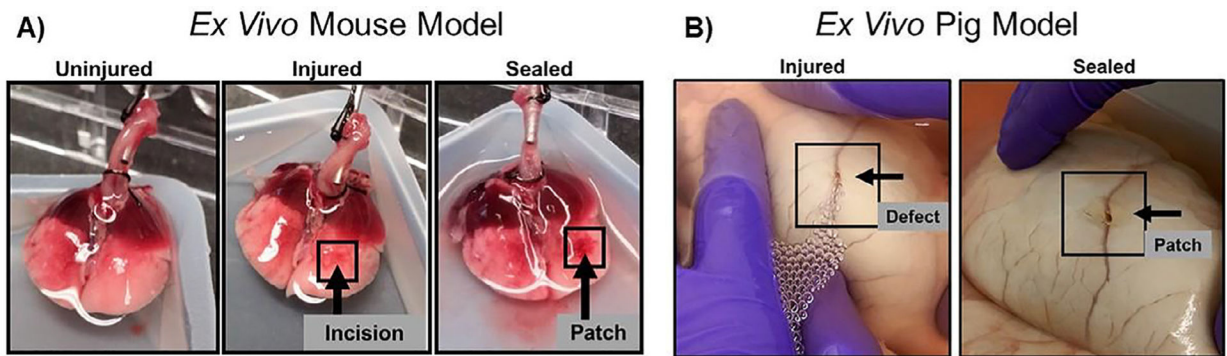


**Fig. 4. Mechanical testing.**

Patches of alginate derivatives and solutions of gelatin derivatives were used. (a) Tensile strength determined by tensile tests. Values represent mean  $\pm$  standard deviation (SD, error bars) and  $n = 6$ . (b) Peel strength by T-peel tests. Values represent mean  $\pm$  SD (error bars) and  $n = 6$ . (c) Shear strength by lap-shear tests. Values represent mean  $\pm$  SD (error bars) and  $n = 6$ . (d) Burst pressure *versus* time to burst (failure). Values represent mean  $\pm$  SD (error bars) and  $n = 5$ . Values represent mean  $\pm$  SD (error bars) of  $n = 4$  from one of two representative experiments. \*  $p < 0.05$ , \*\*  $p < 0.01$ , \*\*\*  $p = 0.0001$ , and \*\*\*\*  $p < 0.0001$ .



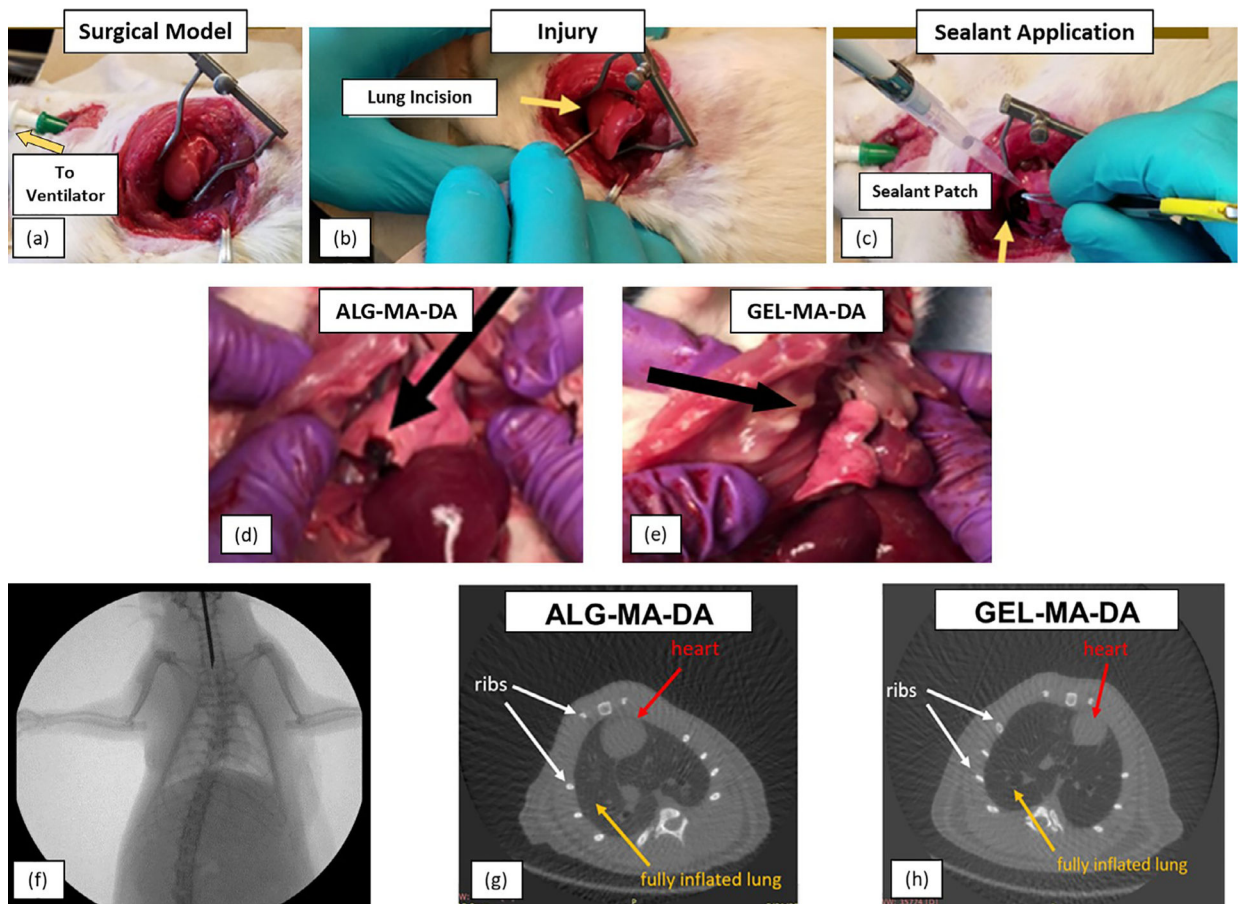
**Fig. 5.** **Cytotoxicity screening** of ALG-MA-DA and GEL-MA-DA sealant materials without (non-polymerized) or following photocrosslinking (polymerized) demonstrate no significant cytotoxicity for human bronchial epithelial (HBE) or transformed alveolar epithelial cells (A549), human pleural mesothelial cells (HPM), or human lung fibroblasts (HLF). (a) In contrast, both the photo-initiator compound and oxidant alone each had significant toxicity on HBE, HPM, and HLF cells. (b) Data is presented as means + SD ( $n = 4$  for each cell line) of similar results from one of two separate experiments. \*\*\*  $p < 0.001$ .



**Fig. 6. Ex vivo lung injury models.**

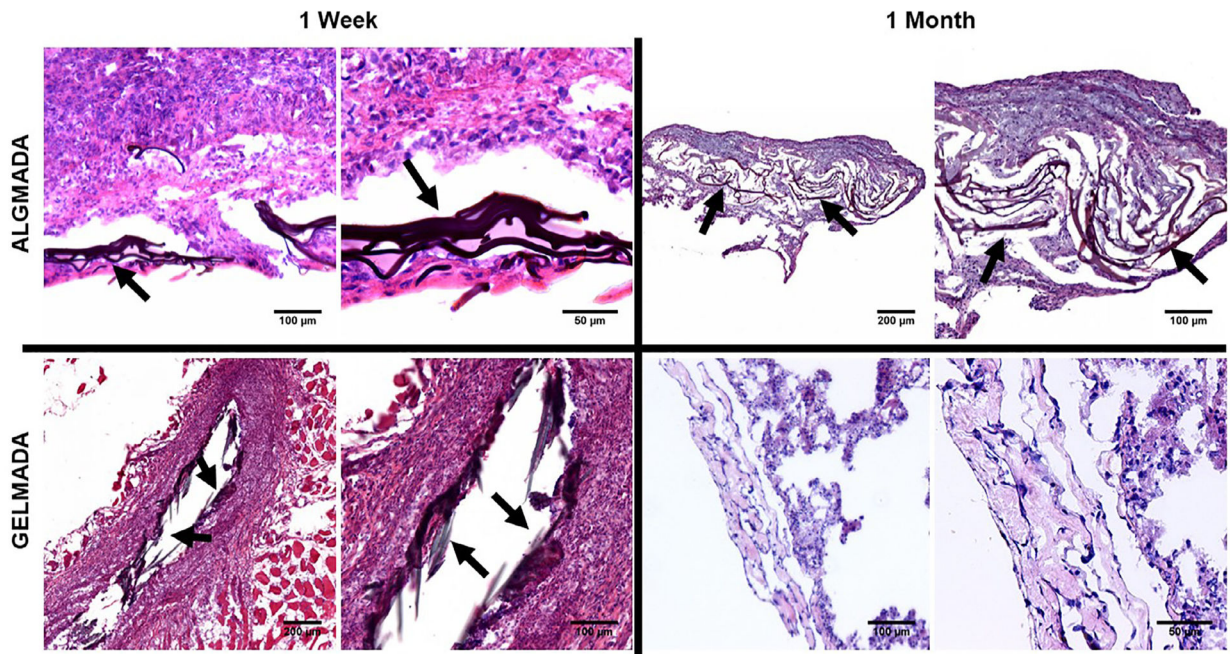
Initial testing of patch adherence and efficacy to seal the defect were performed in ex vivo mouse lung (A) and pig lung (B) models. Arrows determine the position of the defect and the patch. Lungs were inflated and immersed in 1X PBS to visualize the air leak and the seal after patch application.



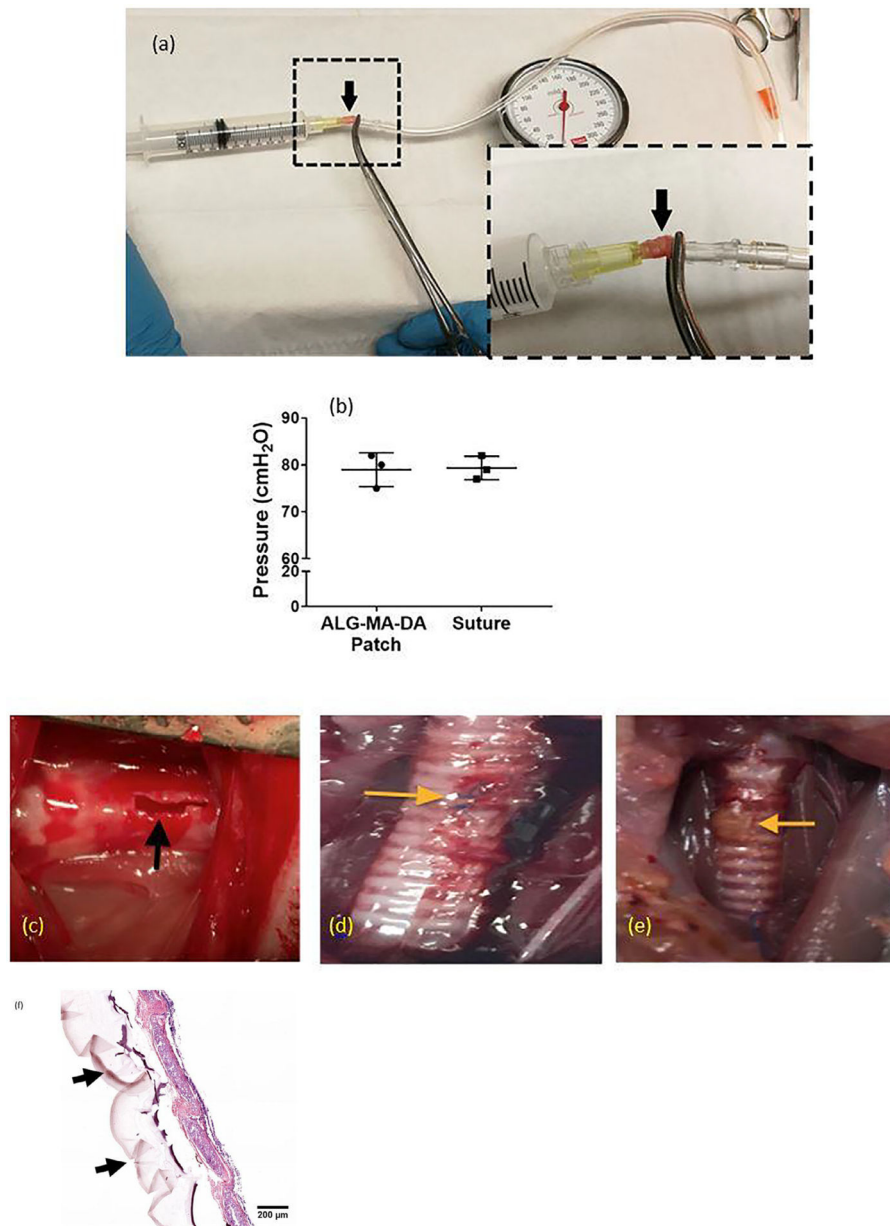


**Fig. 7. *In vivo* model for testing pleural sealant.**

(a) Anesthetized, intubated and mechanically ventilated rats underwent thoracotomy to expose the right lung. (b) Injury is induced by puncture with an 18 g needle and leak of air bubbles observed to confirm injury. (c) The sealant is applied with cessation of air leak. (d) Necropsy of rat 1 week or month post operatively. Residual ALG-MA-DA patch material was observed in rats receiving ALG-MA-DA patch (black arrow). No GEL-MA-DA material was grossly visible in rats receiving GEL-MA-DA *in situ* formed hydrogel application. In neither case was obvious inflammatory reaction or evidence of sealant observed on the parietal pleura/chest wall. High power images are included for panels a-e. (f) Representative fluoroscopy after 1 week demonstrates clear lungs and no obvious pneumothorax. (g) and (h) Representative CT scans at 1 month demonstrates clear lungs and no pneumothorax. White arrows point the ribs; yellow arrows demonstrate a fully inflated lung and red arrows show the position of the heart.



**Fig. 8.** **H and E stained sections** demonstrate good wound repair, no obvious histologic inflammation, and residual sealant (arrows) for 1 week GEL-MA-DA and both 1 week and 1 month ALG-MA-DA. The one week GEL-MA-DA image depicts residual sealant in what appears to be the needle injury tract. Inset depict higher power magnifications of the respective designated areas.

**Fig. 9.**

(a) Set-up for measuring burst pressures in isolated rat trachea. Arrow indicates cannulated rat trachea. (b) Application of the ALG-MA-DA sealant yielded comparable burst pressures to suture control. (c) Exposed rat trachea with scalpel incision (black arrow). (d) Repaired leak with suture at 2 weeks. Yellow arrow indicates residual suture. (e) Repaired leak with ALG-MA-DA patch at 2 weeks. Yellow arrow indicates residual patch. (f) H&E stained cryosection following ALG-MA-DA patch application demonstrates good repair and residual patch material along the tracheal wall (black arrows) Original Mag 200X.